

This article was downloaded by:

On: 14 January 2011

Access details: *Access Details: Free Access*

Publisher *Taylor & Francis*

Informa Ltd Registered in England and Wales Registered Number: 1072954 Registered office: Mortimer House, 37-41 Mortimer Street, London W1T 3JH, UK



## Molecular Simulation

Publication details, including instructions for authors and subscription information:

<http://www.informaworld.com/smpp/title~content=t713644482>

### FT-IR, FT-Raman spectra and DFT vibrational analysis of 2-aminobiphenyl

M. K. Subramanian<sup>a</sup>; P. M. Anbarasan<sup>a</sup>; V. Ilango<sup>b</sup>; N. Sundaraganesan<sup>c</sup>

<sup>a</sup> Department of Physics, Periyar University, Salem, Tamil Nadu, India <sup>b</sup> Department of Physics, Tagore Arts College, Lawspet, Puducherry, India <sup>c</sup> Department of Physics (Engg.), Annamalai University, Chidambaram, India

**To cite this Article** Subramanian, M. K. , Anbarasan, P. M. , Ilango, V. and Sundaraganesan, N.(2008) 'FT-IR, FT-Raman spectra and DFT vibrational analysis of 2-aminobiphenyl', *Molecular Simulation*, 34: 3, 277 – 287

**To link to this Article:** DOI: 10.1080/08927020701829856

**URL:** <http://dx.doi.org/10.1080/08927020701829856>

PLEASE SCROLL DOWN FOR ARTICLE

Full terms and conditions of use: <http://www.informaworld.com/terms-and-conditions-of-access.pdf>

This article may be used for research, teaching and private study purposes. Any substantial or systematic reproduction, re-distribution, re-selling, loan or sub-licensing, systematic supply or distribution in any form to anyone is expressly forbidden.

The publisher does not give any warranty express or implied or make any representation that the contents will be complete or accurate or up to date. The accuracy of any instructions, formulae and drug doses should be independently verified with primary sources. The publisher shall not be liable for any loss, actions, claims, proceedings, demand or costs or damages whatsoever or howsoever caused arising directly or indirectly in connection with or arising out of the use of this material.

## FT-IR, FT-Raman spectra and DFT vibrational analysis of 2-aminobiphenyl

M.K. Subramanian<sup>a</sup>, P.M. Anbarasan<sup>a</sup>, V. Ilango<sup>b</sup> and N. Sundaraganesan<sup>c\*</sup>

<sup>a</sup>Department of Physics, Periyar University, Salem, Tamil Nadu, India; <sup>b</sup>Department of Physics, Tagore Arts College, Lawspet, Puducherry, India; <sup>c</sup>Department of Physics (Engg.), Annamalai University, Annamalai Nagar, Chidambaram, India

(Received 30 August 2007; final version received 24 November 2007)

In this work, the Fourier transform infrared (FT-IR) and Fourier transform Raman (FT-Raman) spectra of 2-aminobiphenyl (2ABP) were recorded in the solid phase. The optimised geometry, frequency and intensity of the vibrational bands of 2ABP were obtained by the density functional theory (BLYP and B3LYP) methods with complete relaxation in the potential energy surface using 6-31G(d) basis set. The harmonic vibrational frequencies were calculated and the scaled values have been compared with experimental FT-IR and FT-Raman spectra. The observed and the calculated frequencies are found to be in good agreement. The experimental spectra also coincide satisfactorily with those of theoretically constructed spectrograms.

**Keywords:** FT-IR and FT-Raman spectra; *ab initio* HF and DFT; 2-aminobiphenyl (2ABP); vibrational analysis

### 1. Introduction

Biphenyl is used as an intermediate in the production of a variety of compounds (e.g. emulsifier, optical brighteners, crop protection products and plastics), as a heat transfer medium in heating fluids, as a dye stuff carrier of textiles and copying papers, as a solvent in pharmaceutical production and in the preservation of citrus fruits. Aromatic amines are widely used as industrial and laboratory reagents. There is a growing interest in examining quantitative structure activity relationships for the genotoxicity of aromatic amines [1].

There is a satisfactory knowledge of the molecular dynamics of the biphenyl molecule [2,3], symmetrically deuterated biphenyls have been synthesised [4] and the infrared and the Raman spectra have been recorded. The syntheses of most of these compounds have been described in literature [5] but very little is known about their vibrational spectra. A large amount of work has been carried on biphenyl and biphenyl- $d_{10}$  by Katon and Lippincott [6], Bree [7], Peregudov [8] and Steele and Lippincott [9]. However, the interpretation of the spectrum does not seem to be completely settled yet. The infrared spectra of some deuterio-derivatives have been reported without any comment in a technical report by Scarborough [10]. The molecular configuration of biphenyl in the solid state was first established more than 30 years ago by the observation that the crystals are monoclinic with two molecules in a unit cell of space group  $P2_1/a$  [11–13]. This necessitates a molecular

centre of symmetry, and hence the two rings must be coplanar. The crystal structure of the biphenyl molecule was investigated by Trotter [14].

To our knowledge, no density functional theory (DFT) calculations and detailed vibrational IR and Raman analysis have been performed on 2-aminobiphenyl (2ABP) molecule. A detailed quantum chemical study will aid understanding of vibrational modes of 2ABP and will clarify the experimental data available for this molecule. DFT calculations are reported to provide excellent vibrational frequencies of organic compounds if the calculated frequencies are scaled to compensate for the approximate treatment of electron correlation, for basis set deficiencies and for the anharmonicity [15–19].

Rauhut and Pulay [20] calculated the vibrational spectra of 31 molecules by using BLYP and B3LYP methods with 6-31G(d) basis set. They reproduced the experimental vibrational frequencies and infrared intensities very well. In their work, they calculated the vibrational frequencies of 20 smaller molecules (the training set), whose experimental vibrational frequencies are well assigned, and derived transferable scaling factors by using the least-square method. The scaling factors are successfully applied to the other 11, larger molecules (the test set). Even when a single scaling factors of 0.995 (0.963) for BLYP(B3LYP) method is employed, root mean square (RMS) deviations for the training and test sets are 26.2 (18.5) and 26.9 (19.7)  $\text{cm}^{-1}$ , respectively. Thus, vibrational frequencies calculated

\*Corresponding author. Email: sundaraganesan\_n2003@yahoo.co.in

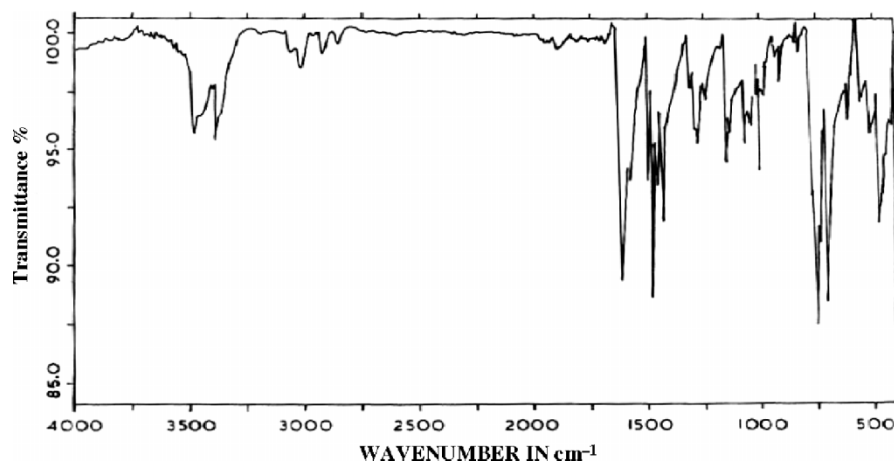


Figure 1. FT-IR spectrum of 2ABP.

by using B3LYP functional with 6-31G(d) basis set can be utilised to eliminate the uncertainties in the fundamental assignments in infrared and Raman vibrational spectra.

In this work, by using DFT (B3LYP and BLYP) methods, we calculate the vibrational frequencies of 2ABP in the ground state to distinguish the fundamentals from the many experimental vibrational frequencies and geometric parameters. These calculations are valuable for providing insight into the vibrational spectrum and molecular parameters.

## 2. Experimental

The compound 2ABP in the solid form was purchased from Sigma-Aldrich Chemical Company (USA) with a stated purity of greater than 98% and it was used as such without further purification. The Fourier transform Raman (FT-Raman) spectrum of 2ABP has been recorded using 1064 nm line of Nd:YAG laser as excitation wave length in the region 100–3500  $\text{cm}^{-1}$  on a Brucker model IFS 66V

spectrophotometer equipped with FRA 106 FT-Raman module accessory. The Fourier transform infrared (FT-IR) spectrum of this compound was recorded in the range of 400–4000  $\text{cm}^{-1}$  on IFS 66V spectrophotometer using KBr pellet technique. The spectrum was recorded at room temperature, with scanning speed of 30  $\text{cm}^{-1} \text{min}^{-1}$  and the spectral resolution of 2  $\text{cm}^{-1}$ . The observed experimental FT-IR and FT-Raman spectra are shown in Figures 1 and 2. Theoretically predicted IR spectra at B3LYP level of calculations are shown in Figure 3. The spectra have been plotted by employing a Lorentzian peak function taking an average width of 10  $\text{cm}^{-1}$ . The spectral measurements were carried out at Sophisticated Analytical Instrumentation Facility, IIT, Chennai.

## 3. Computational details

All the calculations were performed at Hartree–Fock (HF) and B3LYP levels on a Pentium IV/1.6 GHz personal computer using Gaussian 03W [21] program

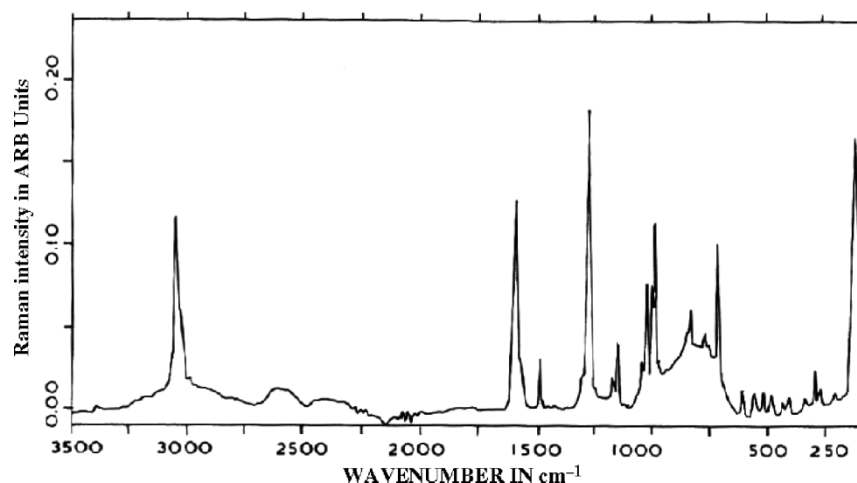


Figure 2. FT-Raman spectrum of 2ABP.

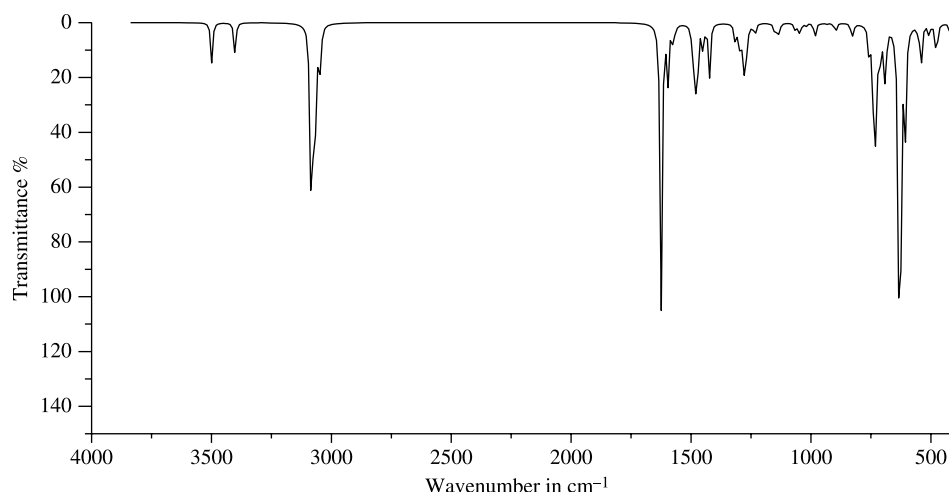


Figure 3. Scaled FT-IR spectrum of 2ABP (B3LYP).

package, invoking gradient geometry optimisation [22]. Initial geometry generated from standard geometrical parameters was minimised without any constraint in the potential energy surface at BLYP level, adopting the standard 6-31G(d) basis set. This geometry was then re-optimised again at B3LYP level, using the same basis set, for better description of polar bonds of amino group. The optimised structural parameters were used in the vibrational frequency calculations at the DFT levels to characterise all stationary points as minima. The 6-31G(d) basis set is employed in the two levels of calculations considered. The smaller basis sets are unreliable and the larger basis sets are expensive. Polarisation functions are necessary to calculate non-planar equilibrium of aniline and its derivatives due to the presence of the amino group's lone pair orbital [23–24]. We have utilised the gradient corrected DFT [25] with the three-parameter hybrid functional (B3) [26] for the exchange part and the Lee–Yang–Parr (LYP) correlation function [27], accepted as a cost-effective approach, for the computation of molecular structure, vibrational frequencies and energies of optimised structures. Vibrational frequencies computed at DFT level have been judged to be more reliable than those obtained by the computationally demanding Moller–Plesset perturbation methods. DFT offers electron correlation frequently comparable to second-order Moller–Plesset theory. Finally, the calculated normal mode vibrational frequencies provide thermodynamic properties also through the principle of statistical mechanics.

By combining the results of the GAUSSVIEW program [28] with symmetry considerations along with available related molecules, vibrational frequency assignments were made with a high degree of accuracy. In order to investigate the performance and vibrational frequencies for the title molecule, mean absolute

deviation, standard deviation (SD), RMS value and correlation coefficient ( $r$ ) between the calculated harmonic and observed fundamental vibrational frequencies for each method and basis set were also calculated and given in Table 4. The RMS values were obtained in this study using the following expression [29].

$$\text{RMS} = \sqrt{\frac{1}{n-1} \sum_{i=1}^n (v_i^{\text{cal}} - v_i^{\text{exp}})^2}.$$

These results indicate that the fundamental frequencies calculated (DFT) for the title compound show quite good agreement with experimental values. Furthermore, the 6-31G(d) basis set calculation approximates the observed fundamental frequencies much better than other basis set results. The small difference between experimental and calculated vibrational modes is observed. This discrepancy can come from the formation of intermolecular hydrogen bonding. Also, we note that the experimental results belong to solid phase and the theoretical calculations belong to gaseous phase.

## 4. Results and discussion

### 4.1 Molecular geometry

The optimised structure parameters of 2ABP calculated by DFT–BLYP and B3LYP levels with the 6-31G(d) basis set are listed in Table 1, in accordance with the atom numbering scheme in Figure 4. All the geometries determined belong to a true minimum proven by real wavenumbers in the vibrational analysis. As seen from Table 1, a general priority for reproducing the experimental bond lengths taken from [14] is not present among BLYP and B3LYP levels. However, all the interatomic distances computed with the DFT–BLYP

Table 1. Geometrical parameters optimised in 2ABP, bond length (Å), bond angle (°) and dihedral angle (°).

Parameters	BLYP/6-31G(d)	B3LYP/6-31G(d)	Experimental <sup>a</sup> (biphenyl)
<i>Bond length (Å)</i>			
C1–C2	1.432	1.419	1.377
C1–C6	1.416	1.405	1.366
C1–N22	1.410	1.400	–
C2–C3	1.415	1.403	1.425
C2–C11	1.497	1.490	1.507
C3–C4	1.403	1.393	1.370
C3–H7	1.094	1.087	1.100
C4–C5	1.406	1.396	1.382
C4–H8	1.093	1.086	1.060
C5–C6	1.400	1.391	1.406
C5–H9	1.094	1.087	0.970
C6–H10	1.096	1.088	1.140
C11–C12	1.418	1.406	1.377
C11–C13	1.419	1.407	1.360
C12–C14	1.404	1.394	1.425
C12–H15	1.094	1.087	1.100
C13–C16	1.405	1.395	1.406
C13–H17	1.093	1.086	1.140
C14–C18	1.406	1.396	1.370
C14–H19	1.095	1.087	1.100
C16–C18	1.406	1.396	1.382
C16–H20	1.095	1.087	0.970
C18–H21	1.094	1.087	1.060
N22–H23	1.022	1.013	–
N22–H24	1.022	1.013	–
<i>Bond angle (°)</i>			
C2–C1–C6	119.12	119.08	120.7
C2–C1–N22	121.66	121.61	–
C6–C1–N22	119.20	119.29	–
C1–C2–C3	118.18	118.37	118.9
C1–C2–C11	122.41	122.23	121.0
C3–C2–C11	119.40	119.39	120.2
C2–C3–C4	122.31	122.22	120.8
C2–C3–H7	118.05	118.11	118.0
C4–C3–H7	119.63	119.66	121.0
C3–C4–C5	118.99	118.94	118.9
C3–C4–H8	120.26	120.30	118.0
C5–C4–H8	120.75	120.76	121.0
C4–C5–C6	120.12	120.15	119.0
C4–C5–H9	120.42	120.39	121.0
C6–C5–H9	119.46	119.46	120.0
C1–C6–C5	121.28	121.24	120.0
C1–C6–H10	118.75	118.79	118.0
C5–C6–H10	119.98	119.97	120.0
C2–C11–C12	120.19	120.21	120.2
C2–C11–C13	121.98	121.79	120.2
C12–C11–C13	117.80	117.98	118.9
C11–C12–C14	121.18	121.11	120.8
C11–C12–H15	119.02	119.07	118.0
C14–C12–H15	119.80	119.82	121.0
C11–C13–C16	120.96	120.90	120.7
C11–C13–H17	119.33	119.31	127.0
C16–C13–H17	119.69	119.78	112.0
C12–C14–C18	120.27	120.23	120.8
C12–C14–H19	119.64	119.67	118.0
C18–C14–H19	120.09	120.10	121.0
C13–C16–C18	120.41	120.37	120.0
C13–C16–H20	119.53	119.56	120.0
C18–C16–H20	120.06	120.07	118.9
C14–C18–C16	119.38	119.42	120.0

Table 1 – continued

Parameters	BLYP/6-31G(d)	B3LYP/6-31G(d)	Experimental <sup>a</sup> (biphenyl)
C14–C18–H21	120.31	120.29	121.0
C16–C18–H21	120.32	120.29	120.0
C1–N22–H23	113.89	113.99	–
C1–N22–H24	114.67	114.77	–
A(23,22,24)	111.50	111.53	–
<i>Dihedral angle (°)</i>			
C6–C1–C2–C3	–0.52	–0.53	–
C6–C1–C2–C11	–179.36	–179.55	–
N22–C1–C2–C3	–178.82	–178.98	–
N22–C1–C2–C11	2.34	2.00	–
C2–C1–C6–C5	0.07	0.11	–
C2–C1–C6–H10	179.91	180.00	–
N22–C1–C6–C5	178.41	178.61	–
N22–C1–C6–H10	–1.75	–1.51	–
C2–C1–N22–H23	–156.18	–156.32	–
C2–C1–N22–H24	–26.04	–25.95	–
C6–C1–N22–H23	25.52	25.22	–
C6–C1–N22–H24	155.66	155.59	–
C1–C2–C3–C4	0.63	0.58	–
C1–C2–C3–H7	179.28	179.36	–
C11–C2–C3–C4	179.50	179.63	–
C11–C2–C3–H7	–1.84	–1.59	–
C1–C2–C11–C12	132.85	131.58	–
C1–C2–C11–C13	–49.10	–50.29	–
C3–C2–C11–C12	–45.97	–47.43	–
C3–C2–C11–C13	132.08	130.70	–
C2–C3–C4–C5	–0.25	–0.21	–
C2–C3–C4–H8	179.28	179.36	–
H7–C3–C4–C5	–178.89	–178.96	–
H7–C3–C4–H8	0.65	0.61	–
C3–C4–C5–C6	–0.22	–0.23	–
C3–C4–C5–H9	–180.00	179.95	–
H8–C4–C5–C6	–179.76	–179.80	–
H8–C4–C5–H9	0.47	0.38	–
C4–C5–C6–C1	0.31	0.27	–
C4–C5–C6–H10	–179.53	–179.61	–
H9–C5–C6–C1	–179.91	–179.90	–
H9–C5–C6–H10	0.25	0.21	–
C2–C11–C12–C14	177.98	178.03	–
C2–C11–C12–H15	–2.91	–2.77	–
C13–C11–C12–C14	–0.15	–0.16	–
C13–C11–C12–H15	178.97	179.04	–
C2–C11–C13–C16	–178.07	–178.12	–
C2–C11–C13–H17	0.55	0.81	–
C12–C11–C13–C16	0.02	0.04	–
C12–C11–C13–H17	178.64	178.98	–
C11–C12–C14–C18	0.22	0.20	–

<sup>a</sup>Taken from [16].

level of theory are greater than the DFT–B3LYP distances. To the best of our knowledge, experimental data on the geometrical parameters of 2ABP are not available in the literature. Therefore, we could not compare the calculation results given in Table 1 with the experimental data. Only optimised geometrical parameters of 2ABP are compared to those of biphenyl [14]. It has been stated in the literature [30] that HF method underestimates bond lengths and that BLYP methods

predict bond lengths which are systematically too long, particularly C–H bond lengths. The B3LYP method leads to geometric parameters which are much closer to experimental data. Because of these reasons we take into account B3LYP/6-31G(d) level for geometric parameters of 2ABP in the present discussion.

The calculated C–C bond lengths in 2ABP molecule are in good agreement with those found in the X-ray structure of biphenyl [14]. For example, in the 2ABP



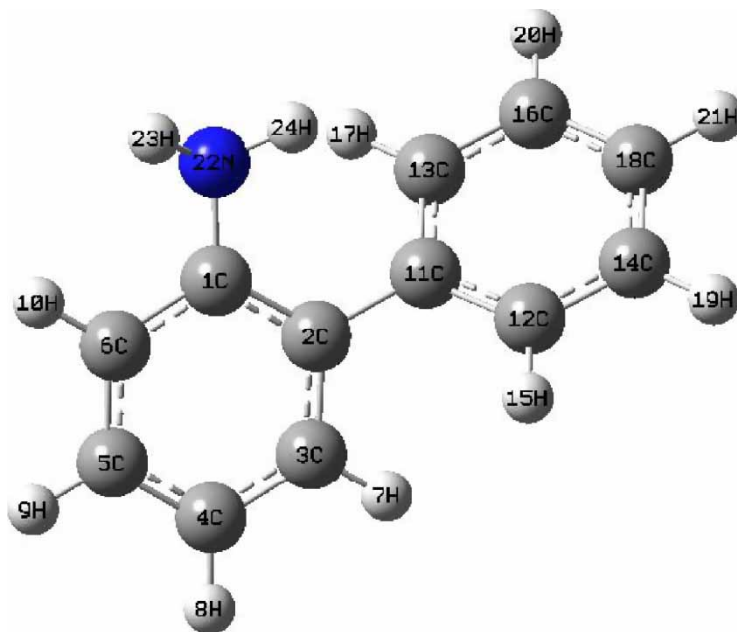


Figure 4. Numbering system adopted in this study (2ABP).

molecule, the first ring C—C bond lengths varies from 1.40 to 1.43 Å by BLYP/6-31G(d) method and 1.39–1.41 Å by B3LYP/6-31G(d) method. For the second ring, the C—C bond lengths varies from 1.40 to 1.42 Å by BLYP/6-31G(d) method and 1.39–1.40 Å by B3LYP/6-31G(d) method.

The benzene ring appears a little distorted with C1—C2 and C1—C6 bond lengths 1.419 and 1.405 Å, respectively, by B3LYP/6-31G(d) exactly at the substitution and rest to the substitution place longer than C3—C4, C4—C5 and C5—C6 bond lengths 1.393, 1.396 and 1.391 Å by the same method. The C2—C1—C6 and C1—C2—C3 angles are calculated as 119, 118° (B3LYP/6-31G(d)) which are smaller than typical hexagonal angle of 120°, respectively. The C2—C3—C4 angle is found to be bigger than the  $\sim 2^\circ$  hexagonal angle. Similar values found to be present in other aniline derivatives which are *o*-methylaniline [31], *m*-methylaniline [32] and *p*-methylaniline [33]. The C1—N bond of *ca.* 1.40 Å by B3LYP method is just 0.03 Å lower than the reported experimental value of 1.43 Å for *p*-methylphenylamine [33].

From the theoretical values, we can find that most of the optimised bond lengths are slightly larger as well as lesser than the experimental values, due to the fact that the calculations have been done on a single molecule in the gaseous state contrary to the experimental values recorded in the presence of intermolecular interactions.

#### 4.2 Vibrational analysis

The molecule of 2ABP consists of 24 atoms, so it has 66 normal vibrational modes. On the basis of a  $C_s$  symmetry

the 66 fundamental vibrations of 2ABP can be distributed as  $21 A'' + 45 A'$ . The  $C_s$  structure was the lowest in energy at all levels. The vibrational bands observed in the infrared region are very sharp, broad and less intense. All these bands have been assigned in terms of various fundamentals, overtone and combination vibrations. Two sets of vibrational frequencies for this molecule are calculated by these methods (BLYP and B3LYP) and then scaled by 0.995 and 0.963 [34], respectively.

#### 4.3 Phenyl ring modes

There are nine CH stretching vibrations observed in both the rings of our compound. The aromatic structure shows the presence of C—H stretching vibrations in the region  $3000\text{--}3100\text{ cm}^{-1}$  which is the characteristic region for the ready identification of C—H stretching vibrations [35]. There are four C—H bonds observed in the first ring, namely C3—H, C4—H, C5—H and C6—H and five C—H bonds are observed in the second ring, namely C12—H, C13—H, C14—H, C16—H and C18—H. The bands observed at 3069, 3023 and  $3009\text{ cm}^{-1}$  in FT-IR and  $3055\text{ cm}^{-1}$  in FT-Raman are attributed to C—H stretching vibrations for both the rings, and this is in excellent agreement with the theoretically computed value by B3LYP/6-31G(d) method of frequency range  $3093\text{--}3051\text{ cm}^{-1}$  (mode nos. 64–56). The strongest Raman line observed at  $3055\text{ cm}^{-1}$  corresponds to the symmetric mode of all C—H bonds in the mono-substituted ring one, as in the case of similar compounds [36].

In di-substituted the C–H in-plane bending mode can be expected in the region  $1000\text{--}1300\text{ cm}^{-1}$ . The bands are sharp but are weak to medium in intensity. The medium and strong intensity bands at 1245, 1175, 1156, 1141, 1070 and  $1024\text{ cm}^{-1}$  in FT-IR spectrum are due to in-plane C–H bendings of both rings. The same vibration appears in the FT-Raman spectrum at 1175, 1158 and  $1027\text{ cm}^{-1}$  with weak as well as medium intensity. The theoretically scaled values of C–H in-plane bending vibrations also fall in the range  $1023\text{--}1236\text{ cm}^{-1}$  (mode nos. 33–41) by B3LYP/6-31G(d) method. The absorption bands arising from C–H out-of-plane bending vibrations are usually observed in the region at  $675\text{--}1000\text{ cm}^{-1}$ . The bands in this region are usually very weak in intensity. The FT-IR bands at 933, 917, 852, 832, 770 and  $735\text{ cm}^{-1}$  and FT-Raman band at  $773\text{ cm}^{-1}$  are assigned to C–H out-of-plane bending vibration. The theoretically computed values of C–H out-of-plane bending vibration also fall in the region  $736\text{--}959\text{ cm}^{-1}$  by B3LYP/6-31G(d) method.

#### 4.4 C–C vibrations

The internal stretching of the C–C bonds appears in both the rings at C1–C2, C2–C3, C4–C5, C5–C6 and at C6–C1 for ring one and C11–C12, C12–C14, C14–C18, C18–C16 and C16–C13 for ring two, while C2–C11 make a bridge between the two benzene rings as shown in Figure 4. The internal stretching coordinates of the C–C bonds in 1st and 2nd ring contribute to 12 modes among the 66 listed in Table 2.

The ring carbon–carbon stretching vibrations occur in the region  $1625\text{--}1430\text{ cm}^{-1}$ . In general, the bands are of variable intensity and are observed at 1625–1590, 1590–1575, 1540–1470, 1465–1430 and  $1380\text{--}1280\text{ cm}^{-1}$  from the frequency ranges given by Varsanyi [37] for the five bands of 1st and 2nd ring in this region. In the present work, the frequencies observed in the FT-IR spectrum at 1580, 1500, 1480, 1453, 1433 and  $1313\text{ cm}^{-1}$  have been assigned to C–C stretching vibrations. The corresponding vibrations appear in the FT-Raman spectrum at  $1500\text{ cm}^{-1}$ . The theoretically scaled values at 1599, 1577, 1567, 1495, 1479, 1452, 1426, 1319 and  $1296\text{ cm}^{-1}$  shows excellent agreement with experimental data by B3LYP/6-31G(d) method.

The very strong band at  $995\text{ cm}^{-1}$  is observed in the FT-Raman spectrum of 2ABP. The corresponding infrared band at  $989\text{ cm}^{-1}$  has a weak intensity. These bands arise from the scaled wavenumber at  $979\text{ cm}^{-1}$  which can be described as the trigonal ring breathing vibration or the ‘star of David’ vibration of aromatic ring [38]. The in-plane deformation vibration is at higher frequencies than the out-of-plane vibrations.

Shimanouchi et al. [39] gave the frequency data for these vibrations for different benzene derivatives as a result of normal coordinate analysis

The C–C–C out-of-plane bending vibrations of both the ring appear in the standard region  $400\text{--}790\text{ cm}^{-1}$  [36]. Six modes have the contribution of bending C–C–C coordinates of both rings. The computed value of C–C–C out-of-plane bending vibration by B3LYP/6-31G(d) method shows at (mode nos. 20, 14-11 and 9) 717, 553–477 and  $404\text{ cm}^{-1}$  shows very good agreement with experimental observations at  $615\text{--}479\text{ cm}^{-1}$  in FT-IR and  $619\text{--}485\text{ cm}^{-1}$  in FT-Raman, respectively.

The C–C–C in-plane bending vibrations observed at 832, 718 and  $703\text{ cm}^{-1}$  in FT-IR, 838 and  $722\text{ cm}^{-1}$  in FT-Raman shows very good agreement with computed values at 707, 609 and  $606\text{ cm}^{-1}$  (mode nos. 19, 16 and 15) by B3LYP/6-31G(d) method.

#### 4.5 Amino group vibrations

The title molecule 2ABP under consideration possesses one  $\text{NH}_2$  group. The  $\text{NH}_2$  group gives rise to the six internal modes of vibrations as the symmetric stretching ( $\nu_s$ ), the anti-symmetric stretching ( $\nu_{as}$ ), the symmetric planar deformation or scissoring ( $\beta_s$ ), the anti-symmetric planar deformation or rocking ( $\beta_{as}$ ), the symmetric non-planar deformation or wagging ( $\omega$ ) and the anti-symmetric non-planar deformation or torsion ( $\tau$ ). The symmetric ( $\nu_s$ ) and anti-symmetric ( $\nu_{as}$ ) stretching modes are easily assigned owing to their characteristic magnitudes in a mono-substituted benzenes. These modes satisfy the following empirical relation, provided the two NH bonds are identical [40].

$$\nu_s = 345.5 + 0.876 \nu_{as}.$$

In all the primary aromatic amines, the N–H stretching frequency occurs in the region  $3300\text{--}3500\text{ cm}^{-1}$  [41]. The asymmetric  $\text{NH}_2$  stretching vibration is computed at  $3505\text{ cm}^{-1}$  by B3LYP/6-31G(d) and  $3503\text{ cm}^{-1}$  by BLYP/6-31G(d) method (mode no. 66) shows good agreement with experimental observations at  $3471\text{ cm}^{-1}$  in FT-IR spectrum. The symmetric stretching vibration is observed at  $3386\text{ cm}^{-1}$  in FT-IR and  $3380\text{ cm}^{-1}$  FT-Raman shows good agreement with computed value at  $3408\text{ cm}^{-1}$  (mode no. 65) by B3LYP/6-31G(d) and  $3404\text{ cm}^{-1}$  by BLYP/6-31G(d) methods. Bellamy and Mancy [42,43] suggested that the  $\text{NH}_2$  scissoring mode lies in the region  $1590\text{--}1650\text{ cm}^{-1}$ . We conclude from the above literature value the strong band of  $1613\text{ cm}^{-1}$  in FT-IR and very strong band of  $1602\text{ cm}^{-1}$  in FT-Raman respectively are assigned to  $\text{NH}_2$  scissoring. While the theoretically computed value by B3LYP/6-31G(d) method at (mode no. 55)  $1627\text{ cm}^{-1}$  shows very good



Table 2. Experimental, BLYP and B3LYP levels computed vibrational frequencies ( $\text{cm}^{-1}$ ) obtained for 2ABP.

Mode no.	Experimental <sup>a</sup>		BLYP/6-31G(d)		Cal I <sub>IR</sub>	Cal I <sub>R</sub>	B3LYP/6-31G(d)		Cal I <sub>IR</sub>	Cal I <sub>R</sub>	Species	Vibrational assignments <sup>b</sup>
	FT-IR	FT-Raman	Computed	Corrected			Computed	Corrected				
1			61	61	7	0	61	59	1	87	A''	Ring torsion
2			84	84	0	0	88	85	2	81	A''	Ring torsion
3		116 vs	114	114	1	0	116	112	11	130	A''	Ring torsion
4		276 w	202	201	0	1	208	201	4	64	A''	$\gamma\text{C}-\text{NH}_2$
5			269	268	4	0	276	266	39	79	A''	Ring deform
6		299 w	292	291	11	0	300	289	20	50	A''	Ring deform
7		338 w	326	324	2	1	333	321	40	6	A''	NH <sub>2</sub> deform
8			360	358	2	1	361	348	5	2	A'	$\rho\text{NH}_2$
9			407	405	0	0	420	404	9	22	A''	$\gamma\text{CCC}$
10		409 w	424	422	22	2	437	421	95	39	A'	$\beta\text{C}-\text{NH}_2$
11	479 s	485 s	481	478	1	5	496	477	54	29	A''	$\gamma\text{CCC}$
12	520 w	522 w	511	509	26	0	528	508	26	2	A''	$\gamma\text{CCC}$
13			544	542	2	1	562	541	19	7	A''	$\gamma\text{CCC}$
14	563 w	560 sh	556	553	2	0	575	553	28	2	A''	$\gamma\text{CCC}$
15			612	609	1	4	629	606	4	2	A'	$\beta\text{CCC} + \beta\text{C}-\text{NH}_2$
16			616	612	9	11	633	609	63	18	A'	$\beta\text{CCC}$
17	615 w	619 w	635	631	11	1	655	631	2	9	A'	$\omega\text{NH}_2$
18	703 vs		694	690	11	0	717	691	8	20	A'	$\beta\text{CCC}$
19	718 w	722 s	710	706	0	1	734	707	1	1	A'	$\beta\text{CCC}$
20	735 w		718	714	15	0	745	717	1	3	A''	$\gamma\text{CCC} + \gamma\text{C}-\text{H}$
21	753 s		736	732	21	0	764	736	1	19	A''	$\gamma\text{CH} + \gamma\text{CCC}$
22	770 w	773 w	759	755	1	1	787	758	0	4	A''	$\gamma\text{CH}$
23			820	816	3	18	849	818	3	1	A''	$\gamma\text{CH}$
24	832 w	838 w	829	825	22	9	861	830	2	2	A'	$\beta\text{CCC}$
25	852 w		835	831	24	0	866	834	37	6	A''	$\gamma\text{CH}$
26			892	887	1	2	931	896	6	1	A''	$\gamma\text{CH} + \gamma\text{CCC}$
27	917 w		902	897	7	190	942	907	50	9	A''	$\gamma\text{CH} + \gamma\text{CCC}$
28			923	918	5	2	966	930	77	2	A''	$\gamma\text{CH}$
29	933 w		931	926	0	4	973	937	20	0	A''	$\gamma\text{CH} + \gamma\text{CCC}$
30			954	950	5	11	995	959	16	1	A''	$\gamma\text{CH}$
31	989 w	995 s	985	980	7	0	1017	979	15	5	A'	Ring breathing (ring 2)
32	1007 m	1008 w	992	987	0	0	1023	985	1	4	A'	Trigonal bending (ring 1)
33	1024 m	1027 m	1029	1024	1	0	1062	1023	3	1	A'	$\beta\text{CH} + \rho\text{NH}_2$
34			1045	1040	0	1	1079	1039	3	1	A'	$\beta\text{CH}$
35	1040 w	1043 w	1060	1055	4	0	1093	1053	10	4	A'	$\rho\text{NH}_2$
36	1070 m		1078	1073	11	0	1111	1069	4	1	A'	$\beta\text{CH}$
37	1141 m		1146	1141	2	1	1178	1134	9	2	A'	t NH <sub>2</sub> + $\beta\text{CH}$
38	1156 m	1158 w	1164	1159	2	1	1193	1149	4	1	A'	$\beta\text{CH}$
39			1167	1161	0	0	1195	1151	5	3	A'	$\beta\text{CH}$
40	1175 w	1175 w	1185	1179	22	2	1216	1171	3	5	A'	$\beta\text{CH}$
41	1245 w		1245	1239	1	5	1284	1236	6	2	A'	$\beta\text{CH}$
42			1263	1256	26	0	1307	1259	5	1	A'	$\nu\text{C2}-\text{C11}$
43	1283 w	1284 s	1289	1282	2	1	1326	1277	1	3	A'	$\nu\text{C}-\text{NH}_2 + \nu\text{CC}$

Table 2 – continued

Mode no.	Experimental <sup>a</sup>		BLYP/6-31G(d)		Cal I <sub>IR</sub>	Cal I <sub>R</sub>	B3LYP/6-31G(d)		Cal I <sub>IR</sub>	Cal I <sub>R</sub>	Species	Vibrational assignments <sup>b</sup>
	FT-IR	FT-Raman	Computed	Corrected			Computed	Corrected				
44			1312	1306	2	0	1346	1296	1	19	A'	$\nu$ CC
45	1313 w		1330	1324	1	4	1364	1314	0	4	A'	$\nu$ CC + t NH <sub>2</sub>
46			1338	1332	9	11	1370	1319	3	1	A'	$\nu$ CC
47	1433 m		1435	1428	11	1	1481	1426	2	2	A'	$\nu$ CC
48	1453 w		1461	1453	11	0	1508	1452	37	6	A'	$\nu$ CC
49	1480 s		1488	1480	0	1	1536	1479	6	1	A'	$\nu$ CC
50	1500 m	1500 w	1500	1492	15	0	1552	1495	50	9	A'	$\nu$ CC
51			1564	1556	8	0	1627	1567	77	2	A'	$\nu$ CC
52			1572	1564	1	1	1637	1577	20	0	A'	$\nu$ CC
53			1594	1586	3	18	1660	1599	16	1	A'	$\nu$ CC
54	1580 w		1599	1591	12	9	1662	1600	15	5	A'	$\nu$ CC + $\delta$ NH <sub>2</sub>
55	1613 s	1602 vs	1640	1632	84	0	1690	1627	104	4	A'	$\delta$ NH <sub>2</sub>
56	3009 w		3081	3065	1	2	3169	3051	3	1	A'	$\nu$ CH
57	3023 w		3092	3076	7	190	3179	3062	3	1	A'	$\nu_{as}$ CH
58		3055s	3098	3082	5	2	3185	3067	10	4	A'	$\nu_{as}$ CH
59			3100	3084	0	4	3187	3069	4	1	A'	$\nu_{as}$ CH
60			3106	3091	9	11	3193	3075	9	2	A'	$\nu_{as}$ CH
61			3111	3096	3	18	3198	3080	4	1	A'	$\nu_{as}$ CH
62			3119	3104	15	9	3206	3087	5	3	A'	$\nu_{as}$ CH
63			3124	3108	24	0	3211	3092	3	5	A'	$\nu_s$ CH
64	3069 m		3126	3110	1	319	3212	3093	6	343	A'	$\nu_s$ CH
65	3386 w	3380 vw	3421	3404	7	190	3539	3408	5	1	A'	$\nu_s$ NH <sub>2</sub>
66	3471 w		3521	3503	5	2	3640	3505	6	2	A'	$\nu_{as}$ NH <sub>2</sub>

<sup>a</sup> s, strong; vs, very strong; m, medium; w, weak; vw, very weak; sh, shoulder; <sup>b</sup>  $\nu$ , stretching;  $\nu_s$ , sym. stretching;  $\nu_{as}$ , asym. stretching;  $\beta$ , in-plane-bending;  $\gamma$ , out-of-plane bending;  $\omega$ , wagging;  $\rho$ , rocking;  $t$ , twisting;  $\tau$ , torsion;  $I_{IR}$ , IR intensities;  $I_R$ , Raman scattering activities.

agreement with experimental observations, compared with BLYP/6-31G(d) method. It is noted that the frequency of scissoring mode of  $\text{NH}_2$  group is observed in the vicinity of spectral range of ring stretching modes (8a or 8b) but as always having higher magnitude than these modes. The anti-symmetric (rocking) mode appears in the range  $1000\text{--}1100\text{ cm}^{-1}$  with variational IR intensity. In the present case this mode is assigned at  $1040\text{ cm}^{-1}$  in FT-IR and  $1043\text{ cm}^{-1}$  in FT-Raman spectra. The scaled value at  $1053\text{ cm}^{-1}$  by B3LYP/6-31G(d) method exactly coincides with experimental observation.

The  $\text{C}\text{--}\text{NH}_2$  stretching vibration are observed as a weak band at  $1283\text{ cm}^{-1}$  in FT-IR and  $1284\text{ cm}^{-1}$  as a very strong band in FT-Raman shows good agreement with computed value at  $1277\text{ cm}^{-1}$  by B3LYP/6-31G(d) method.

The  $\text{C}\text{--}\text{NH}_2$  in-plane bending vibration are observed at  $409\text{ cm}^{-1}$  in FT-Raman also shows very good agreement with computed value by B3LYP/6-31G(d) method at  $421\text{ cm}^{-1}$ . The  $\text{C}\text{--}\text{NH}_2$  out-of-plane bending vibration is observed at  $276\text{ cm}^{-1}$  in FT-Raman deviating positively by  $\sim 75\text{ cm}^{-1}$  when compared with the B3LYP/6-31G(d) method. As we note that both  $\text{C}\text{--}\text{NH}_2$  in-plane and out-of-plane bending vibration are absent in FT-IR. The  $\text{NH}_2$  wagging computed at  $631\text{ cm}^{-1}$  (mode no. 17) by B3LYP/6-31G(d) method shows good agreement with experimental spectrum at  $615$  and  $619\text{ cm}^{-1}$  in FT-IR and FT-Raman respectively. The frequency observed at  $1141\text{ cm}^{-1}$  in FT-IR are assigned to  $\text{NH}_2$  twisting vibration shows deviation of about  $\sim 7\text{ cm}^{-1}$  with computed value at  $1134\text{ cm}^{-1}$  (mode no. 35) by B3LYP/6-31G(d) method.

## 5. Other molecular properties

Several calculated thermodynamic parameters are presented in Table 3. Scale factors have been

Table 3. Theoretically computed energies (a.u.), zero-point vibrational energies ( $\text{kcal mol}^{-1}$ ), rotational constants (GHz), entropies ( $\text{cal mol}^{-1}\text{ K}^{-1}$ ) and dipole moment (D) for 2ABP.

Parameters	BLYP/6-31G(d)	B3LYP/6-31G(d)
Total energy	−518.4196446	−518.6588885
Zero-point energy	120.91	124.72
Rotational constants	1.8608	1.8896
	0.5187	0.5256
	0.4325	0.4399
Entropy		
Total	100.35	99.25
Translational	41.28	41.28
Rotational	31.00	30.98
Vibrational	28.04	26.99
Dipole moment	1.405	1.345

Table 4. Mean absolute deviation, SD,  $r$  and RMS between the calculated and observed fundamental vibrational frequencies of the title compound.

	BLYP/6-31G(d)	B3LYP/6-31G(d)
Mean absolute deviation	7.5000	9.1764
SD	6.8824	6.4419
RMS	10.1792	11.2118
$r$	0.9999	0.9998

recommended [44] for an accurate prediction in determining the zero-point vibration energies (ZPVE), and the entropy,  $S_{\text{vib}}(T)$ . The variations in the ZPVEs seem to be insignificant. The total energies and the changes in the total entropy of 2ABP at room temperature at different methods also presented.

## 6. Conclusion

The FT-IR and FT-Raman spectra have been recorded and the detailed vibrational assignment is presented for 2ABP for the first time. The harmonic vibrational frequencies, IR intensities, Raman scattering activities and IR spectra of 2ABP were determined and analysed both at DFT–BLYP and B3LYP/6-31G(d) levels of theory. The difference between the corresponding wave numbers (observed and calculated) is very small, for most of fundamentals. Therefore the results presented in this work for 2ABP indicates that this level of theory is reliable for prediction of both infrared and Raman spectra of the title compound. The optimised geometry parameters calculated at BLYP/6-31G(d) are slightly larger than those calculated at B3LYP/6-31G(d) level and the B3LYP calculated values coincide well compared with the experimental data on the whole (Table 4).

## References

- [1] Z. You et al., *Ortho-substituted effects on the vitro and in vivo genotoxicity of benzidine derivatives*, Mutat. Res. 319 (1993), p. 19.
- [2] G. Zerbi and S. Sandroni, *Vii European Congress on Molecular Spectroscopy*, Budapest, July (1963).
- [3] K. Krep, S. Sandroni, and G. Zerbi, *Flow-frequency vibration of crystalline biphenyl*, J. Chem. Phys. 40 (1964), p. 3502.
- [4] F. Geiss, S. Sandroni, and G. Blech, *Zur synthese und analyse deuterierter Bi-und Terphenyle*, J. Label. Comp. 3(4) (1967), p. 271.
- [5] R.J. Akawie, J.M. Scarborough, and J.G. Burr, *Synthesis of deuterated biphenyls*, J. Org. Chem. 24 (1959), p. 946.
- [6] J.E. Katon and E.R. Lippincott, *The vibrational spectra and geometrical configuration of biphenyl*, Spectrochim. Acta 15 (1959), p. 627.
- [7] A. Bree, C.Y. Pang, and L. Rabeneck, *The Raman spectrum of biphenyl and biphenyl- $d_{10}$* , Spectrochim. Acta 27A (1971), p. 1293.

- [8] G.V. Peregudov, *Calculation and interpretation of the vibrational spectra of biphenyl and some of its deuterium substitution products*, Opt. Spectrosc. 9 (1960), p. 155.
- [9] D. Steele and E.R. Lippincott, *The crystal and solution vibrational spectra of biphenyl*, J. Mol. Spectrosc. 6 (1961), p. 238.
- [10] J.M. Scarborough, Technical report NAA-SR-4657, Atomic International.
- [11] G.L. Clark and L.W. Pickett, *Crystal structures of some derivatives of diphenyl*, Proc. Nat. Acad. Sci. USA 16 (1930), p. 20.
- [12] ———, *X-ray investigation of optically active compounds. II. Diphenyl and some of its active and inactive derivatives*, J. Am. Chem. Soc. 53 (1931), p. 167.
- [13] J. Dhar, *X-ray analysis of the structure of biphenyl*, Ind. J. Phys. 7 (1932), p. 43.
- [14] J. Trotter, *The crystal and molecular structure of biphenyl*, Acta Cryst. 14 (1961), p. 1135.
- [15] N.C. Handy, C.W. Murray, and R.D. Amos, *Study of methane, acetylene, ethane, and benzene using Kong-Sham theory*, J. Phys. Chem. 97 (1993), p. 4392.
- [16] P.J. Stephens et al., *Ab initio calculation of vibrational absorption and circular dichroism spectra using density functional force fields*, J. Phys. Chem. 98 (1994), p. 11623.
- [17] F.J. Devlin et al., *Ab initio calculation of vibrational absorption and circular dichroism spectra using density functional force fields: A comparison of local nonlocal, and hybrid density functionals*, J. Phys. Chem. 99 (1995), p. 16883.
- [18] S.Y. Lee and B.H. Boo, *Density functional theory study of vibrational spectra of anthracene neutral and radical cation*, Bull. Korean Chem. Soc. 17 (1996), p. 754.
- [19] ———, *Molecular structure and vibrational spectra of 9-fluorenon density functional theory study*, Bull. Korean Chem. Soc. 17 (1996), p. 760.
- [20] G. Rauhut and P. Pulay, *Transferable scaling factors of density functional derived vibrational force fields*, J. Phys. Chem. 99(10) (1995), p. 3093.
- [21] M.J. Frisch et al., Gaussian, Inc., Wallingford, CT (2004).
- [22] H.B. Schlegel, *Optimization of equilibrium geometric and transition structures*, J. Comput. Chem. 3 (1982), p. 214.
- [23] Y. Wang, S. Saebo, and C.U. Pittman, Jr., *The structure of aniline by ab initio studies*, J. Mol. Struct. (Theochem) 281 (1993), p. 91.
- [24] M. Gorse and A. Pesquer, *A theoretical study of aniline and some derivatives in their ground states*, J. Mol. Struct. (Theochem) 281 (1993), p. 21.
- [25] P. Hohenberg and W. Kohn, *Inhomogeneous electron gas*, Phys. Rev. 136 (1964), p. B864.
- [26] A.D. Becke, *Density-functional thermochemistry. III. The role of exact exchange*, J. Chem. Phys. 98 (1993), p. 5648.
- [27] C. Lee, W. Yang, and R.G. Parr, *Development of the Colle-Salvetti correlation-energy formula into a functional of electron density*, Phys. Rev. B 37 (1988), p. 785.
- [28] A. Frisch, A.B. Nielson, and A.J. Holder, *GAUSSVIEW User Manual*. Gaussian Inc., Pittsburgh, PA, 2000.
- [29] V. Krishnakumar et al., *Analysis of vibrational spectra of 4-amino-2,6-dichloropyridine and 2-chloro-3,5 dinitropyridine based on the density functional theory calculations*, Spectrochim. Acta 65A (2006), p. 147.
- [30] M. Kurt, M. Yurdakul, and S. Yurdakul, *Molecular structure and vibrational spectra of 3-chloro-4-methyl aniline by density functional theory and ab initio Hartree Fock calculations*, J. Mol. Struct. (Theochem) 711 (2004), p. 25.
- [31] A.K. Goluk and M. Kumru, *Theoretical and experimental studies of the vibration spectra of m-methylaniline*, J. Mol. Struct. 625 (2003), p. 17.
- [32] W.B. Tzeng et al., *Structures and vibrations of o methylaniline in the  $S_0$  and  $S_1$  states studies by ab initio calculations and resonant two-photon ionization spectroscopy*, Spectrochim. Acta 55A (1998), p. 153.
- [33] W.B. Tzeng and K. Narayanan, *Structures and vibrations of p-methyl aniline in the  $S_0$  and  $S_1$  states studied by ab initio calculations and resonant two-photon ionization spectroscopy*, J. Mol. Struct. 446 (1998), p. 93.
- [34] M. Kurt and S. Yurdakul, *Computational note on molecular structure and vibrational spectra of 6-and 8-methylquinoline molecules by quantum mechanical methods*, J. Mol. Struct. 804 (2007), p. 75.
- [35] V. Krishnakumar and V. Balachandar, *FTIR and FT-Raman spectra, vibrational assignments and density functional theory calculations of 2, 6 dibromo-4-nitroaniline and 2-(methylthio) aniline*, Spectrochim. Acta 61A (2005), p. 1811.
- [36] G. Varsanyi, *Vibrational Spectra of Benzene Derivatives*, Academic Press, New York, 1964.
- [37] ———, *Vibrational Spectra of Benzene Derivatives*, Academic Press, New York, 1969.
- [38] F.R. Dollisn, W.G. Fateley, and F.F. Bentley, *Characteristic Raman Frequencies of Organic Compounds*, Wiley, New York, 1974, pp. 170–175.
- [39] T. Shimanouchi, Y. Kakiuti, and I. Gamo, *Out-of-plane CH vibrations of benzene derivatives*, J. Chem. Phys. 25 (1956), p. 1245.
- [40] L.J. Bellamy and R.L. Williams, *The NH stretching frequencies of primary amines*, Spectrochim. Acta 9 (1957), p. 341.
- [41] R. Wysokinski et al., *Density functional study on the molecular structure, infrared and Raman spectra, and vibrational assignment of 4-thiocarbamoylpyridine*, J. Mol. Struct. 791 (2006), p. 70.
- [42] L.J. Bellamy, *The Infrared Spectra of Complex Molecules*, Vol. 2, Chapman and Hall, London, 1980.
- [43] S. Mancy, W.L. Peticoles, and R.S. Toblas, *Raman spectra of methyl derivatives of 5' adenosine monophosphate, tubercidine, inosin, uridine and cytidine. Perturbation of nucleoside vibrations of electrophilic attack at different sites*, Spectrochim. Acta 35A (1979), p. 315.
- [44] M. Alcolea Palafox, *Scaling factors for the prediction of vibrational spectra I benzene molecule*, Int. J. Quant. Chem. 77 (2000), p. 661.